INFECTION AND IMMUNITY, June 2006, p. 3125–3133 Vol. 74, No. 6
0019-9567/06/$08.00+0 doi:10.1128/IAI.02061-05

Mycobacterium marinum Erp Is a Virulence Determinant Required for Cell Wall Integrity and Intracellular Survival

Christine L. Cosma,[1]* Kathryn Klein,[1]† Rosa Kim,[1] Dana Beery,[1] and Lalita Ramakrishnan[1,2,3]

Departments of Microbiology,[1] Immunology,[2] and Medicine,[3] University of Washington, Seattle, Washington 98195

Received 21 December 2005/Returned for modification 8 February 2006/Accepted 7 March 2006

The *Mycobacterium tuberculosis* exported repetitive protein (Erp) is a virulence determinant required for growth in cultured macrophages and in vivo. To better understand the role of Erp in *Mycobacterium* pathogenesis, we generated a mutation in the *erp* homologue of *Mycobacterium marinum*, a close genetic relative of *M. tuberculosis*. *erp*-deficient *M. marinum* was growth attenuated in cultured macrophage monolayers and during chronic granulomatous infection of leopard frogs, suggesting that Erp function is similarly required for the virulence of both *M. tuberculosis* and *M. marinum*. To pinpoint the step in infection at which Erp is required, we utilized a zebrafish embryo infection model that allows *M. marinum* infections to be visualized in real-time, comparing the *erp*-deficient strain to a ΔRD1 mutant whose stage of attenuation was previously characterized in zebrafish embryos. A detailed microscopic examination of infected embryos revealed that bacteria lacking Erp were compromised very early in infection, failing to grow and/or survive upon phagocytosis by host macrophages. In contrast, ΔRD1 mutant bacteria grow normally in macrophages but fail to induce host macrophage aggregation and subsequent cell-to-cell spread. Consistent with these in vivo findings, *erp*-deficient but not RD1-deficient bacteria exhibited permeability defects in vitro, which may be responsible for their specific failure to survive in host macrophages.

Mycobacteria, typified by *Mycobacterium tuberculosis*, are intracellular pathogens that cause persistent infections despite vigorous host responses (13), and much of the work aimed at understanding mycobacterial pathogenesis has focused on the interactions between mycobacteria and the immune system. The infectious process can be viewed as a series of sequential steps, in which the bacteria interface with the immune system in multiple complex ways. Infection begins with the recruitment of macrophages to the site of infection and phagocytosis of infecting organisms. These infected macrophages then migrate to deeper tissues, and additional monocytes are recruited to the infected cell. As bacterial growth ensues, macrophages aggregate and differentiate into the characteristic epithelioid macrophages that constitute granulomas. Later, as adaptive immunity develops, other immune cells such as lymphocytes are recruited to the granulomas. The bacterium-host interactions that orchestrate this complex program are not well understood, and the bacterial determinants that permit both early growth and long-term persistence are now being identified.

The last decade has seen significant advancements in the genetic manipulation of mycobacteria to define and characterize mycobacterial virulence factors (13, 24, 32, 41). Mutations that reduce virulence have been identified, and the majority of these affect the structure and/or the function of the highly complex cell wall and outer lipid layer. These include mutations in genes involved in cell wall lipid synthesis, composition, or transport (8, 9, 11, 14, 19, 20, 22, 23, 28); the PGRS cell surface proteins (2, 36, 39); and the RD1 locus that encodes a putative secretion system (21, 25, 26, 31, 35, 45). However, a clear understanding of the underlying mechanisms for these virulence deficiencies has been lacking.

The *Mycobacterium* protein Erp, another cell surface component, was the first *Mycobacterium* virulence protein to be characterized by targeted deletion (4). Despite a series of genetic and biochemical characterizations (5, 16, 17, 29, 30), its role in virulence remains poorly understood. This *Mycobacterium*-specific secreted/cell surface protein is comprised of three domains: a conserved N-terminal domain with a canonical Sec-dependent signal sequence, a repetitive central domain, and a conserved hydrophobic C-terminal domain that appears to be involved in a loose anchoring of Erp to the cell surface (30). Virulence studies with *M. tuberculosis* and *M. bovis erp* mutants revealed that the bacteria are growth attenuated in cultured macrophages and in a mouse model of infection (4, 5).

M. marinum, a close genetic relative of *M. tuberculosis* (43) (http://www.sanger.ac.uk/Projects/M_marinum/), is used as a model for mycobacterial pathogenesis (3, 15, 18, 21, 22, 33, 34, 42). *M. marinum* is the causative agent of systemic granulomatous infections of ectotherms, such as fish and frogs (1), and peripheral chronic granulomatous disease (fish tank granulomas) in humans (44). Experimental inoculation of leopard frogs (*Rana pipiens*) results in a chronic subclinical infection much like latent tuberculosis in humans (37). Given that *M. tuberculosis* and *M. marinum* cause similar pathology in infected hosts, have similar endocytic trafficking pathways in cultured macrophages (3), and share virulence determinants (21, 45), it is likely that these related pathogens use similar survival strategies in vivo.

We have previously developed a zebrafish embryo model of infection to characterize the earliest events after mycobacterial infection (15). Zebrafish embryos are transparent during the first 2 weeks of life, allowing the infectious process to be visualized in real time. Studies using this model revealed that

* Corresponding author. Mailing address: Department of Microbiology, University of Washington, Seattle, WA 98195. Phone: (206) 221-6367. Fax: (206) 616-4286. E-mail: ccosma@washington.edu.

† Present address: Centers for Molecular Medicine, State University of New York—Stony Brook, Stony Brook, NY 11794-5120.

M. marinum injected into the bloodstream are rapidly taken up by host macrophages, usually within 30 min of injection. Over the next 24 h, infected macrophages exit the bloodstream, migrating into tissues. These infected macrophages next begin to aggregate and further recruit additional uninfected macrophages, some of which ultimately differentiate into the epithelioid macrophages typical of granulomas. The timing of aggregation, although dependent on both the virulence of the strain used and the number of organisms injected, usually occurs 2 to 5 days postinjection (J. M. Davis and L. Ramakrishnan, unpublished results). This system has proven valuable in clarifying the mechanism of action of *Mycobacterium* virulence determinants. For example, in a previous study we demonstrated that the *M. marinum* ΔRD1 mutant (45), like its *M. tuberculosis* counterpart, is growth attenuated when assayed by bacterial counts in bulk-cultured macrophages. However, detailed analysis using the zebrafish embryo infection model showed that RD1-deficient bacteria are capable of growth in individual macrophages in vivo but fail to induce macrophage aggregation and subsequent intercellular spread (45). This finding revealed that intracellular growth in individual macrophages is insufficient to ensure bacterial proliferation and that additional host cells must be recruited and infected.

In the present study, we characterize another *M. marinum* virulence determinant, the *erp* locus, using a combination of in vivo and in vitro assays. We found that, like the *M. marinum* RD1 locus, *erp* is required for bacterial growth in vivo. However, by using the zebrafish embryo model, we show that, in contrast to the RD1 locus, *erp* is required for growth and/or survival in individual macrophages. The growth attenuation of this mutant in vivo may be explained at least in part by a permeability defect.

MATERIALS AND METHODS

Bacterial strains and growth conditions. Mycobacterial strains used for the present study were derived from a human clinical isolate, strain M (ATCC BAA-535) and are shown in Table 1. *M. marinum* was grown in Middlebrook 7H9 broth (Difco) supplemented with 0.5% bovine serum albumin, 0.005% oleic acid, 0.2% glucose, 0.2% glycerol, 0.085% sodium chloride, and 0.05% Tween 80 or on Middlebrook 7H10 agar (Difco) supplemented with 0.5% bovine serum albumin, 0.005% oleic acid, 0.2% glucose, 0.2% glycerol, and 0.085% sodium chloride. Media were supplemented with 20 μg of kanamycin/ml and 50 μg of hygromycin/ml when appropriate. pGFPHYG2 was obtained by inserting the hygromycin resistance cassette of plasmid pRF498H (40) into the NsiI sites of plasmid pMSP12::GFP (10), thus disrupting the kanamycin resistance cassette.

Construction of the *M. marinum erp* mutant. A 2,857-bp PstI/BglI fragment containing the *erp* locus was isolated from a *M. marinum* genomic cosmid library and inserted into pBluescript SK(+) (Stratagene). The *erp* gene was interrupted by removing a central 316-bp SmaI fragment and replacing it with the *aph* (kanamycin resistance) cassette of pYUB213 (a gift from W. Jacobs) to generate an *erp*::*aph* mutation. The *sacB* gene was then introduced at the XbaI site of the polylinker, and the resulting plasmid, pERPKO, was used to transform *M. marinum* strain M. Kanamycin-resistant (Kan^r) $sucrose^s$ merodiploid colonies were isolated and streaked onto medium containing kanamycin and sucrose to select for $sucrose^r$ double recombinants. One such isolate was saved and named KK33 (Table 1). Complementation of *erp*::*aph* was achieved by cloning a 2,284-bp NruI/MscI fragment containing the wild-type allele into pYUB178Hyg to generate pERPcomp1, which was then transformed into KK33 and integrated into the *att* site to produce strain KK60 (Table 1). The presence of the knockout and the complementing alleles were confirmed by Southern blot analysis (data not shown).

Macrophage infections. Growth in J774 macrophages was determined as described previously (36). Briefly, 5×10^4 J774A.1 murine macrophages in grown in Dulbecco modified Eagle medium (Gibco) supplemented with 10% fetal bovine serum were seeded into the wells of a 24-well plate and allowed to adhere overnight. The following day, the cells were infected with *M. marinum* for 1 h at 33°C. Infected medium was replaced with 1 ml of fresh medium containing 40 μg of streptomycin/ml. To determine the intracellular bacterial counts at various times postinfection, cells were washed three times with 1× phosphate-buffered saline, lysed with 100 μl of 1% Triton X-100, scraped with a pipette tip, and diluted 10-fold with 1× phosphate-buffered saline. Dilutions were plated onto 7H10 agar and incubated at 33°C for 7 to 14 days.

TABLE 1. Bacterial strains used in this study

Strain	Relevant genotype	Source or reference
M	ATCC BAA-535	37
RD1-6	M ΔRD1	45
KK33	M *erp*::*aph*	This study
KK60	KK33 with erp^+ integrated at *att* site	This study
4E4	M *kasB*::Kan^r	22
4E4-comp	4E4 with integrated $kasB^+$ allele	22
KK11	M/pGFPHYG2	This study
KK47	KK33/pGFPHYG2	This study
CC59	RD1-6/pGFPHYG2	This study

Frog infection. Wild-caught male *Rana pipiens* (approximately 10 to 12 cm) were obtained from J. M. Hazen (Alberg, VT). Frogs were infected by intraperitoneal injection as described previously (12). One, two, or twelve weeks later, liver and spleen tissues were harvested, and the bacterial CFU were enumerated by plating on 7H10 agar supplemented with amphotericin B and, in the case of KK33 and KK60, with kanamycin. Frogs were housed and all animal procedures were carried out in accordance with University of Washington IACUC regulations.

Zebrafish procedures. Zebrafish embryos at 32 h postfertilization were infected by microinjection at the caudal vein as previously described (12, 15). To assess virulence of various *M. marinum* strains, cohorts of embryos hatched at the same time were infected (45 embryos per strain) and monitored daily for mortalities. Each treatment group of 45 embryos was distributed into three tanks of fifteen and scored separately to account for the possible contribution of tank effects. Mean time to death (MTD) was scored for each tank, and no significant differences were found between tanks of fish infected with the same strain. The data for fish infected with a given strain were then pooled, and MTD values between strains were compared by using analysis of variance (ANOVA). For the visualization of bacteria in vivo, fluorescent strains were used (Table 1), and embryos were mounted for observation as described previously (12, 15, 45). When scoring the levels of infection in zebrafish embryos, the individual making this assessment was blinded to the strain used to infect each embryo so as to avoid bias.

MIC assays. The agar dilution method was used to determine the MIC for each strain (22). Individual plates of 7H10 agar (supplemented as described above) were prepared (30-ml volume), with twofold dilutions of the antibiotic being tested. Plates were spotted with 10 μl of early-log-phase cultures in triplicate, and all strains were spotted onto the same plate. Plates were incubated at 33°C and scored after 8 and 11 days.

Statistical analyses. Statistical analysis was performed by using In-Stat software (Graphpad Software, Inc.).

RESULTS

Targeted deletion of the *M. marinum erp* locus. We compared the previously identified *M. marinum erp* locus (17) (http://www.sanger.ac.uk/Projects/M_marinum/) with its *M. tuberculosis* homologue and found an overall 76% amino acid identity and 81% similarity. *M. marinum erp* is located between the *glf* and *csp* open reading frames, making its genomic arrangement syntenous with those of other *Mycobacterium* species. The central repetitive domain of the predicted protein contains two additional PGLTS repeats compared to that of *M. tuberculosis* (17), making it the closest identified homologue to those of the *M. tuberculosis* complex. A BLAST search of the completed *M. marinum* genome sequence failed to identify any

additional open reading frames with homology to the *M. tuberculosis erp* sequence, suggesting that *M. marinum* contains only one *erp* allele. To investigate the role of *erp* in *M. marinum* pathogenesis, we generated a loss-of-function mutation by introducing a Kan^r cassette via homologous recombination near the end of the N-terminal domain (see Materials and Methods). This mutation was complemented by introducing the wild-type *erp* allele at the *att* site (Table 1). As in the case of the *M. tuberculosis erp* mutant (4), growth of the *M. marinum erp*::*aph* mutant strain in liquid culture was similar to that of the wild type (data not shown). However, growth on 7H10 agar was mildly compromised since *erp*::*aph* mutant colonies appeared 3 days later than did the wild type. A small colony phenotype has been reported for *erp*-deficient mutants in other species (30).

The *M. marinum erp* mutant is growth attenuated in cultured macrophages and adult animals. The *M. tuberculosis erp* locus is required for growth both in cultured macrophages and in a mouse model of infection (4). We found *M. marinum erp* to be similarly required for growth in cultured macrophages. As shown in Fig. 1A, the *erp*::*aph* strain failed to grow in J774A.1 macrophages over an 8-day time course. This growth attenuation was indistinguishable from that observed for a *M. marinum* mutant that lacks the RD1 virulence locus (45). In contrast, the wild-type and complemented mutant strains grew approximately 50-fold over the 8-day monitoring period.

To examine whether *erp*-deficient bacteria were also attenuated in vivo, we assayed their growth in a natural host species, the leopard frog, used to study *M. marinum* pathogenesis in the laboratory (6, 37). Intraperitoneal infection of frogs with wild-type bacteria resulted in an increased tissue burden over a period of 12 weeks (Fig. 1B). In contrast, the number of *erp*::*aph* mutant bacteria decreased slightly, and by 12 weeks postinfection it was 1.5 logs below that of the wild type ($P < 0.05$). ΔRD1 mutant bacteria were similarly attenuated ($P < 0.05$), as shown previously (45). As was the case in cultured macrophages, complementation of the *erp*::*aph* mutation restored growth in frogs. Thus, the *M. marinum* and *M. tuberculosis erp*-deficient mutants had comparable phenotypes with respect to growth in culture, macrophage monolayers, and animals. Furthermore, the attenuation characteristics of the *M. marinum erp*-deficient mutant were indistinguishable from those of the *M. marinum* ΔRD1 mutant (31, 45).

The *M. marinum erp*::*aph* mutant is attenuated in the zebrafish embryo infection model. The *M. marinum erp*::*aph* mutant was next analyzed for virulence in the zebrafish embryo infection model (15). In this model, embryos are infected by microinjection with a small number of bacteria (ranging from 10 organisms to ~300) at approximately 32 h postfertilization, shortly after the beginning of circulation. Injection directly into the caudal vein results in immediate dispersal of the bacteria via the bloodstream, their subsequent uptake by circulating macrophages, and migration of infected macrophages into the tissues where they aggregate to form granulomas. To assess the virulence of the *erp*::*aph* mutant, 45 embryos were infected per strain, and survival was monitored over a 2-week time course. Embryos infected with the *erp*::*aph* and ΔRD1 mutants fared better than those infected with wild-type and *erp*::*aph* complemented strains (Fig. 2A). The MTD for embryos infected with

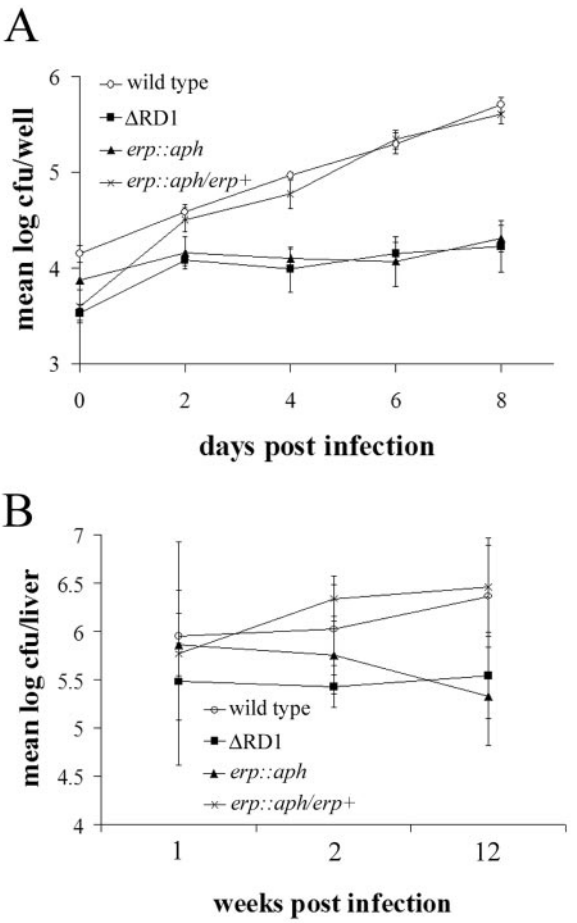

FIG. 1. The *M. marinum erp*::*aph* mutant is growth attenuated in both murine macrophages and frogs. (A) J774A.1 macrophages were infected as described in Materials and Methods with strains M (○, 8.8×10^3 CFU), KK33 (▲, 7.7×10^3 CFU), KK60 (×, 4.4×10^3 CFU), or RD1-6 (■, 1.6×10^4 CFU). All datum points were obtained in triplicate, and the means and standard deviations are shown. The assay was performed two additional times with similar results. (B) Leopard frogs ($n = 5$) were infected as described in Materials and Methods with strain M (○, 6.7×10^5 CFU), KK33 (▲, 2.9×10^5 CFU), KK60 (×, 2.5×10^5 CFU), or RD1-6 (■, 2.7×10^5 CFU). Mean log CFU per liver are shown with the standard deviation, and the Students unpaired *t* test was used to assess significance. For the 2-week time point, $P < 0.05$ (KK33 versus KK60). For the 12-week time point, $P < 0.05$ (M versus RD1-6 and M versus KK33) and $P < 0.01$ (KK33 versus KK60). Similar results were obtained from the spleen (data not shown).

the wild-type and complemented strains was significantly shorter than for those infected with the mutants (Table 2).

To determine whether these differences in embryo survival resulted from differential growth of the bacteria in vivo, we undertook a microscopic analysis of embryos infected with wild-type and mutant bacteria expressing *gfp* from a strong constitutive promoter (see Table 1 and Materials and Methods). Ten embryos were injected per strain and were viewed by fluorescence microscopy 1 h later to verify that the inocula were similar and then again at 5 days postinoculation to examine the degree of bacterial proliferation. As shown in Fig. 2B, the overall burden of bacteria was similar for all embryos at 1 h postinfection, but by 5 days postinfection wild-type-

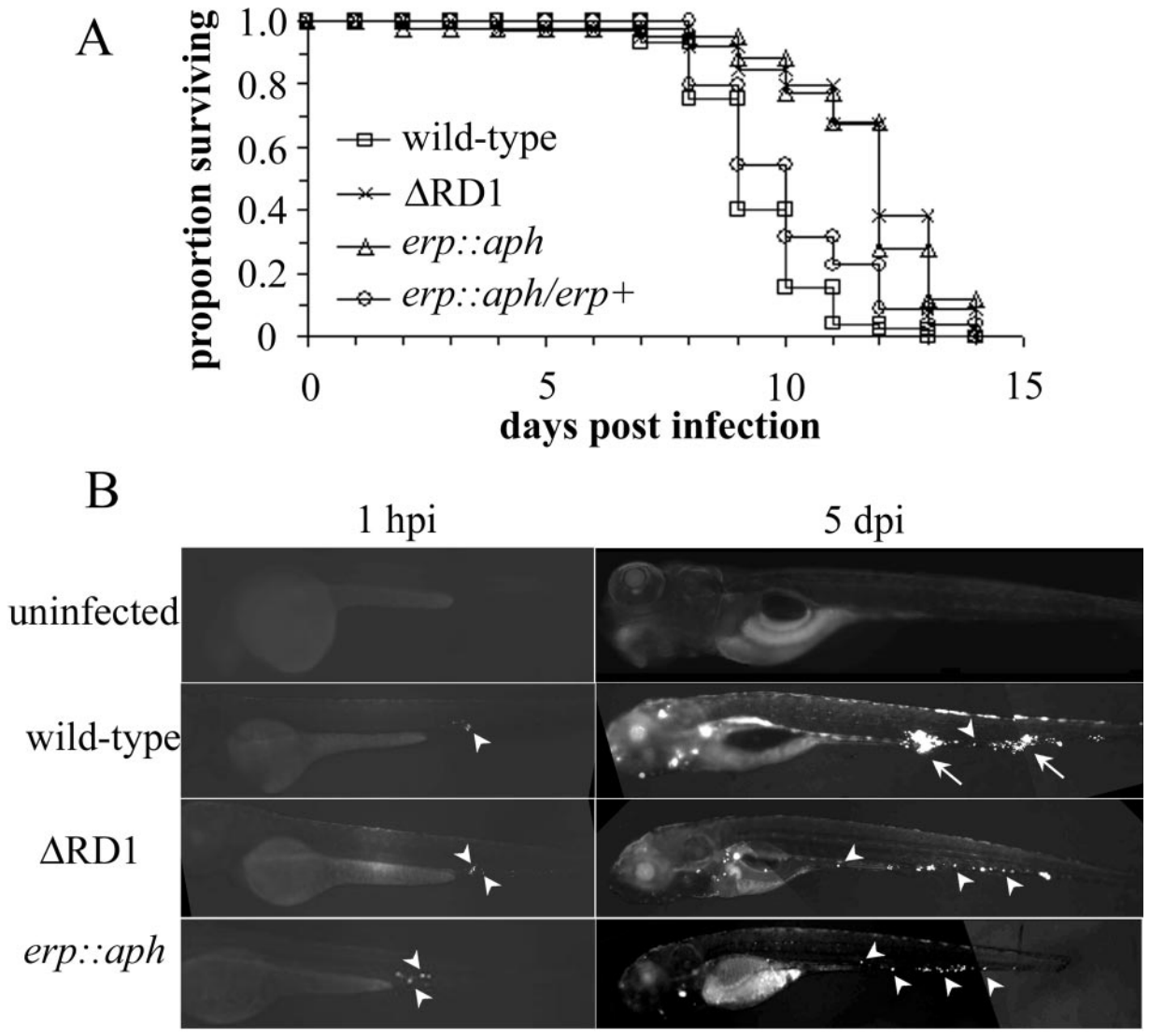

FIG. 2. *erp*::*aph* and ΔRD1 mutants exhibit reduced virulence and growth in zebrafish embryos. (A) Kaplan-Meier curves for zebrafish embryos infected with the following doses (CFU): strain M (20 CFU), KK33 (38 CFU), RD1-6 (22 CFU), and KK60 (53 CFU). The data are shown as percent surviving each day postinfection. (B) Embryos were infected with the following doses (CFU): KK11 (161 CFU), CC59 (200 CFU), and KK47 (226 CFU). Embryos were imaged at both 1 h and at 5 days postinfection by using a fluorescence microscope at ×40 total magnification. Images shown are 10-s exposures of green fluorescence. Some autofluorescence is visible along the dorsal side due to the presence of melanophores.

infected embryos harbored more bacteria than embryos infected with *erp*::*aph* or ΔRD1 bacteria. Injection with either of these strains resulted in low burden infections and a paucity of macrophage aggregates typical of the wild-type infection (Fig. 2B, arrows). We could not quantify the growth of these strains in zebrafish embryos using bacterial counts, since we were unable to recover *erp*::*aph* mutant bacteria using the lysis procedure required for this analysis (45). This failure to recover *erp*::*aph* mutant bacteria was specific as wild-type and ΔRD1 bacteria were readily recovered (H. Volkman, D. Beery, and L. Ramakrishnan, unpublished data). These experiments revealed that *erp*::*aph* and ΔRD1 bacteria were similarly growth attenuated in zebrafish embryos.

TABLE 2. Mean time to death for zebrafish embryos infected with *M. marinum*[a]

Strain	MTD (SD) in days	*P*
M	9.3 (0.61)	
RD1-6	11.6 (0.90)	<0.001
KK33	11.5 (0.59)	<0.001
KK60	10.0 (0.30)	NS

[a] Embryos were infected as described for Fig. 2A. *P* values (versus strain M) were determined by using ANOVA. NS, not significant.

Erp-deficient bacteria fail to grow intracellularly in a zebrafish embryo model of infection. The intracellular growth by mycobacteria has traditionally been assayed in cultured cell lines by enumerating the total growth of the bacterial population in a population of macrophages as a surrogate measure of growth in the individual cells. However, recent studies of the

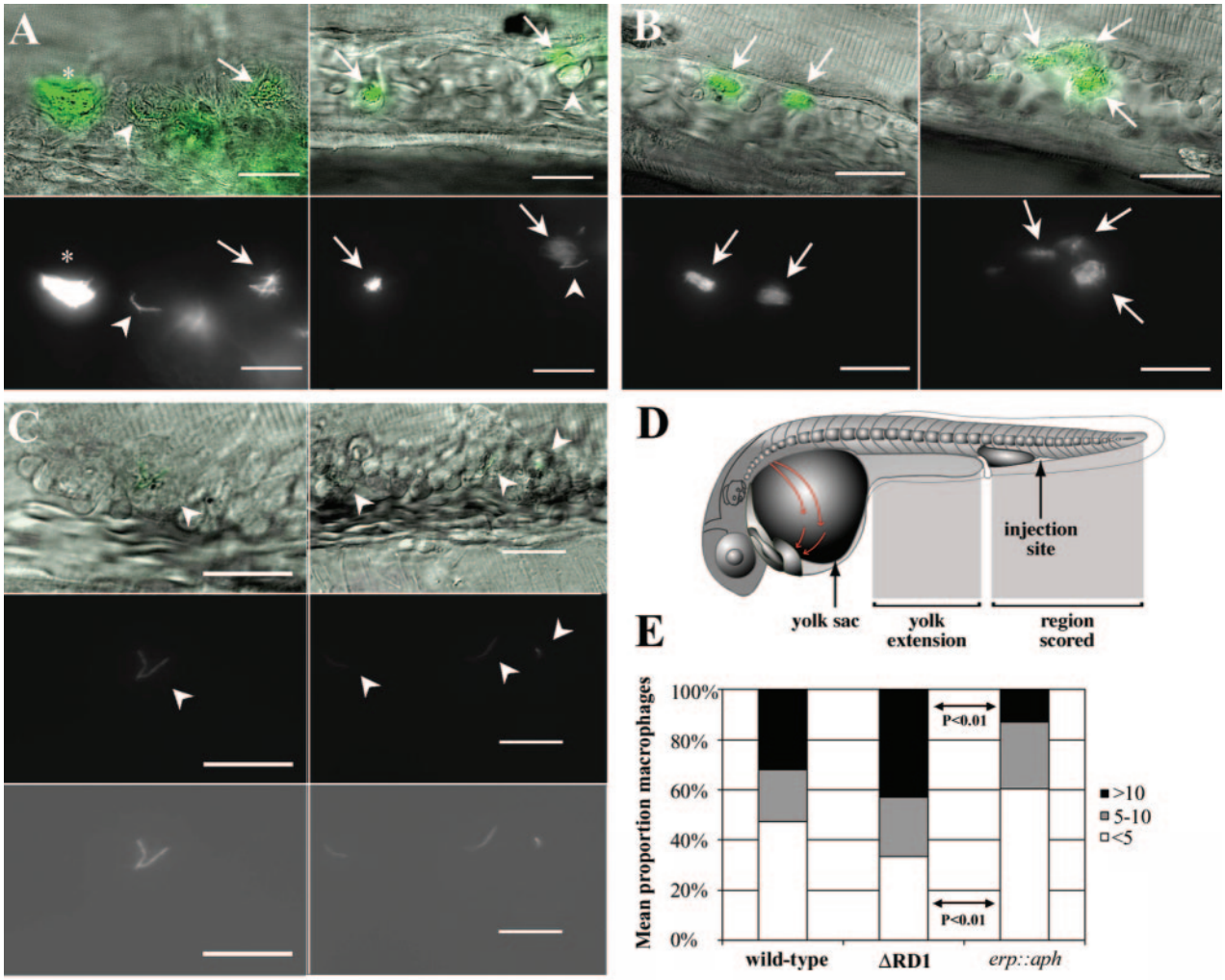

FIG. 3. *erp*::*aph* mutant bacteria fail to grow or survive in zebrafish embryo macrophages. Ten embryos were infected per strain and were examined by fluorescence and DIC microscopy at 5 days postinfection at ×600 magnification. Mean infection doses (CFU) were as follows: KK11 (158 CFU), CC59 (214 CFU), and KK47 (279 CFU). Shown are representative images of infected macrophages for KK11 (A), CC59 (B), and KK47 (C). For each panel, upper images are overlays of DIC (grayscale) and bacterial fluorescence (green), while bottom images are fluorescence only. Scale bar, 25 μm. Arrows indicate heavily infected macrophages, arrowheads indicate lightly infected macrophages, and the asterisk indicates an aggregate of infected macrophages. For the bottom panels of panel C, the brightness and contrast were adjusted to allow better visualization of KK47 bacteria, which were dimmer than the other strains. (D) Schematic diagram of the zebrafish embryo. (E) Average proportion of macrophages containing <5, 5 to 10, or >10 bacteria, when embryos were infected with wild-type, ΔRD1, or *erp*::*aph* bacteria. Significance was assessed by ANOVA, comparing the proportion in each category across the three strains. The mean number of individual infected macrophages did not differ between strains. See the text for additional details.

RD1 locus (21, 25, 45) have shown that this can be a faulty assumption. In our previous work we found that ΔRD1 bacteria seemingly failed to grow intracellularly (as measured in such an assay); however, closer examination using the zebrafish embryo model revealed that these bacteria are capable of intracellular growth but rather fail to spread among host cells. We concluded that in intracellular growth assays in cultured cell lines, a limited amount of growth may occur intracellularly, but unless bacteria continue to spread to new host cells, no increase in the overall population is observed. Therefore, we were similarly interested to use this infection model to pinpoint the precise nature of attenuation for the *erp*::*aph* mutant.

Prior detailed analyses in the zebrafish embryo have revealed that infection by wild-type bacteria proceeds in sequential steps (15). Upon injection of *M. marinum*, macrophages migrate to the site of infection and phagocytose the bacteria. Infected macrophages then migrate back into tissues and ultimately aggregate into granulomas. In initial experiments with the *erp*::*aph* strain we did not observe any obvious defects in macrophage recruitment, phagocytosis of bacteria, or migration into tissues (D. Beery and L. Ramakrishnan, unpublished observations), suggesting that, like the ΔRD1 mutant (45), the *erp*::*aph* mutant was competent for these very early steps. We next performed a detailed comparison of embryos infected with wild-type, ΔRD1, and *erp*::*aph* bacteria at 5 days postinfection by using fluorescence and differential interference contrast (DIC) microscopy at high magnification. Similar to what was observed at low magnification (Fig. 2B), abundant macro-

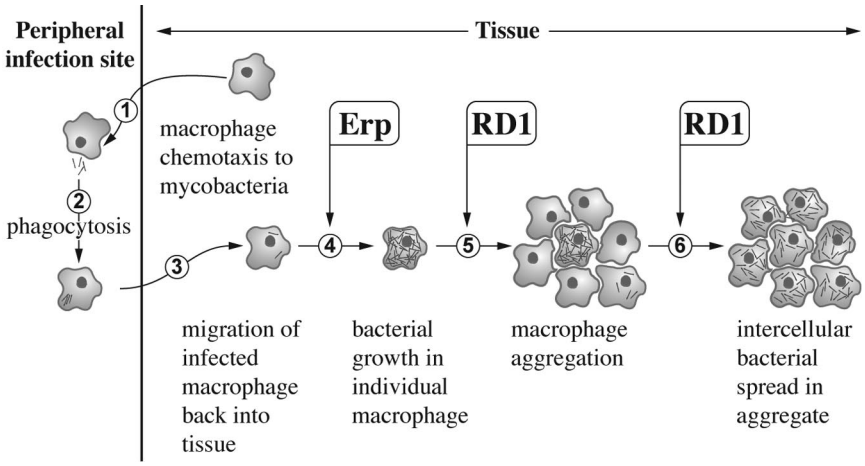

FIG. 4. Proposed pathway for the early stages of *Mycobacterium* pathogenesis, highlighting the steps impacted by the Erp and RD1 virulence determinants. See the text for details.

phage aggregates were found in the wild-type-infected embryos, whereas fewer were observed in embryos infected with either mutant strain (data not shown). With respect to the infection burden of individual (nonaggregated) macrophages, wild-type-infected embryos contained macrophages representing a wide spectrum of infection levels, as expected. Single macrophages contained anywhere from one to >10 bacteria (Fig. 3A). However, a striking difference was apparent between embryos infected with the two mutant strains. Macrophages of embryos infected with the ΔRD1 mutant typically harbored large numbers of bacteria (Fig. 3B), whereas those from embryos infected with the *erp*::*aph* mutant frequently harbored very few bacteria (Fig. 3C). Furthermore, *erp*::*aph* bacteria were often dim (Fig. 3C), suggesting that they are being killed (in contrast, all strains were similarly bright in culture). These observations suggested that *erp*::*aph* and ΔRD1 mutant bacteria might be attenuated for distinct reasons, despite their similarities in other assays.

To quantify the observed differences, we studied 10 infected embryos for each of the three strains. For each embryo, the entire region posterior to the end of the yolk extension (Fig. 3D) was surveyed, and individual (nonaggregated) infected macrophages found in this region were scored. Each macrophage was scored based on the number of bacteria it contained; <5 bacteria, 5 to 10 bacteria, or >10 bacteria. For each embryo, we calculated the proportion of its macrophages that were lightly infected (<5 bacteria), moderately infected (5 to 10 bacteria), and heavily infected (>10 bacteria). Consistent with the qualitative findings (Fig. 3A to C), we observed that significantly more infected macrophages fell into the high-burden category (>10 bacteria per cell) when the embryos were infected with ΔRD1 bacteria than when they were infected with *erp*::*aph* bacteria ($P < 0.01$). The converse was also true; significantly more infected macrophages fell into the low-burden category (<5 bacteria per cell) when the embryos were infected with *erp*::*aph* bacteria than when they were infected with ΔRD1 bacteria ($P < 0.01$). No difference was observed in the proportions of moderately infected macrophages. Wild-type-infected embryos had an intermediate number of macrophages in each category. This was due to the fact that during infection by wild-type bacteria, infected macrophages are titrated out into granulomas, which were not scored in this assay. In contrast, the ΔRD1 and *erp*::*aph* mutant-infected macrophages were less likely to form aggregates, and the discrepancy in the number of bacteria they contained reveals that these two mutant strains are attenuated for different reasons despite their identical attenuation phenotypes in virulence assays that measure overall organism burden (Fig. 1). *erp*-deficient bacteria are attenuated primarily because of their lack of intracellular growth and/or survival, whereas ΔRD1 mutant bacteria grow successfully in macrophages but fail to induce subsequent aggregation and intercellular spread (Fig. 4) (45).

Erp is required for the *Mycobacterium* permeability barrier. As discussed above, we specifically failed to recover *erp*::*aph* mutant bacteria extracted from zebrafish embryos. The extraction method requires that embryo lysates be plated on 7H11 agar in the presence of polymixin B, trimethoprim, and carbenecillin to suppress the growth of intestinal and other aquatic flora (H. Volkman and L. Ramakrishnan, unpublished). Since *erp*::*aph* bacteria were clearly present (as visualized by fluorescence microscopy, Fig. 2B), we suspected that they might simply be more susceptible to the antimicrobial compounds in the agar. Therefore, we determined the MIC for wild-type and mutant bacteria of a panel of antimicrobial compounds. As a control we included an *M. marinum* strain that contains a transposon insertion in *kasB*, a gene required for mycolate synthesis (22). *kasB*-deficient bacteria are more permeable to the hydrophobic detergent deoxycholate, and are consequently more susceptible to a variety of lipophilic antibiotics such as rifampin and erythromycin, but retain normal susceptibility to hydrophilic compounds. As shown in Table 3, the *erp*::*aph* mutant strain was more susceptible to the lipophilic antibiotics rifampin, erythromycin, and chloramphenicol than were the wild-type and complemented strains. The degree of sensitivity was similar to that observed for *kasB*-deficient strain and was in contrast to the ΔRD1 strain, which demonstrated normal susceptibility. These findings suggest that the *M. marinum* *erp*::*aph* mutant has increased permeability to a variety of hy-

TABLE 3. *erp*-deficient bacteria are more susceptible to hydrophobic antibiotics

Strain	MIC (μg/ml)[a]					
	STR	RIF	ERY	CAM	PMB	INH
M	8	0.32	64	256	>1,600	8
RD1-6	8	0.32	64	256	>1,600	8
KK33	4	0.04	2	32	400	8
KK60	8	0.32	32	256	>1,600	8
4E4	4	0.02	<1	32	200	8
4E4-comp	8	0.32	64	256	>1,600	8

[a] The MIC was measured as described in Materials and Methods. Plates were incubated at 33°C for 8 to 11 days prior to scoring. The MIC was determined as the minimum concentration that prevented the appearance of any growth. The results of a typical experiment are shown. Antibiotic abbreviations: STR, streptomycin sulfate; RIF, rifampin; ERY, erythromycin; CAM, chloramphenicol; PMB, polymixin B; INH, isoniazid.

drophobic agents, which may explain its decreased growth and/or survival in macrophages.

DISCUSSION

In the present study, we have characterized the role of the *M. marinum erp* gene during infection. Like its *M. tuberculosis* and *M. bovis* counterparts (4, 5), we find that *M. marinum* Erp is a virulence determinant, required for growth in cultured macrophages and in vivo. In this regard, our findings add to a growing body of evidence that the molecular determinants of *M. tuberculosis* virulence during infection of mammals are also used by *M. marinum* during infection of its natural hosts (7, 21, 36, 39, 45). That Erp function is conserved among mycobacteria is further supported by studies in *M. tuberculosis* showing that the *erp* loci of *M. leprae* and *M. smegmatis* are competent for complementation of an *M. tuberculosis erp* mutation in the context of a mouse infection (16). Such commonalities suggest that the basic mechanisms of *Mycobacterium* pathogenesis are conserved.

As was the case with the RD1 locus (45), the zebrafish embryo infection model has refined our understanding of the role of the *erp* locus in *Mycobacterium* virulence. Using this model we find that Erp-deficient bacteria have an early and intrinsic defect in intracellular growth and/or survival in macrophages. This is in contrast to ΔRD1 bacteria, which proliferate normally in individual macrophages but have diminished and delayed formation of macrophage aggregates and are defective in intercellular spread within these aggregates (45). This difference in intracellular growth was not revealed in the standard assay designed to monitor net bacterial growth in a population of cultured macrophages (Fig. 1A) but rather was observed only when a detailed comparison of the two mutants was made during infection of zebrafish embryos (Fig. 3). The points at which these two determinants impact the infectious process are depicted in Fig. 4. Although both begin to exert their influence in the early stages of infection, it is clear that *erp* is required earlier than is the RD1 locus. Erp-deficient bacteria do not survive or grow within individual macrophages, so that infection is thwarted prior to macrophage aggregation into granulomas. It is noteworthy that the differences in the capacity of these two mutants for intracellular growth do not result in a differential outcome later in infection (Fig. 1B and 2A and Table 2). This observation reinforces our previous findings with the ΔRD1 mutant that the capacity for intracellular growth alone is not sufficient to confer full virulence and that the ability of mycobacteria to proliferate to their maximum extent also depends on the cell-to-cell spread impacted by the RD1 locus. Furthermore, it would appear that these two aspects of the infectious process (intracellular growth and intercellular spread) are important throughout infection, since both mutants are comparably attenuated in the short-term embryo infection model and in the long-term chronic frog model. That both mutants are capable of establishing infection, albeit at a lower tissue burden than for the wild type, reinforces the notion that mycobacteria use multiple redundant mechanisms to ensure their survival (9, 14, 36, 39).

The finding that the *erp*::*aph* mutant is compromised for intracellular growth, coupled with its failure to grow on Middlebrook 7H11 agar replete with antibiotics, suggested a permeability defect that might explain both phenotypes. Indeed, upon further examination we found that the loss of Erp renders bacteria more permeable to a variety of lipophilic compounds. These permeability defects may render the bacteria more susceptible to intracellular host defenses such as reactive oxygen and nitrogen intermediates, degradative enzymes, and defensins. Permeability defects have been postulated as the reason for attenuation for a variety of *Mycobacterium* mutants. For example, mutations in the *M. marinum kasB* gene involved in mycolate production rendered bacteria more permeable to deoxycholate and more sensitive to a variety of lipophilic antibiotics (22). On the other hand, mutations in the *M. tuberculosis fadD26* and *mmpL7* genes, which are involved in PDIM synthesis (8, 9, 14), rendered bacteria more permeable to detergent (38) and yet not more susceptible to hydrophobic antibiotics (19, 38). Clearly, the complexity of the permeability barrier conferred by the *Mycobacterium* cell wall and outer lipid layer are such that individual components may confer protection against different types of compounds.

That permeability defects are complex is further revealed by a comparison of the attenuation phenotypes of various permeability mutants. In *M. tuberculosis*, the *fadD26* mutant is growth attenuated in activated, but not naive macrophages (38), whereas macrophage activation is not required to restrict growth of *erp* mutants (4; the present study). Indeed, some permeability mutants do not have a virulence defect, as is the case with the *M. tuberculosis fbcC* gene, which encodes a mycolyltransferase (27). In *M. marinum*, the *erp* and *kasB* mutants have similar profiles of susceptibility to lipophilic antibiotics (22; the present study) (Table 3), and yet the former is more attenuated for growth in cultured macrophages (22; C. Cosma and L. Ramakrishnan, unpublished data). In our preliminary examination of the *kasB* mutant in zebrafish embryos, we found that in this model too, *kasB*-deficient bacteria are less attenuated than *erp*::*aph* bacteria (Cosma, Kim, and Ramakrishnan, unpublished). These differences in intracellular growth could be for several reasons. First, features of the *Mycobacterium* permeability barrier relevant for intracellular survival may simply not be revealed by in vitro membrane permeability assays. Alternatively, the permeability defect conferred by the loss of Erp may be only partially responsible for its virulence defects and Erp may play a second role in intracellular survival, independent of its contribution to the *Myco-*

bacterium permeability barrier. Finally, the loss of KasB may have a severe enough effect on the *Mycobacterium* cell wall or outer lipid layer that genetic or regulatory compensations have occurred to provide better survival both in vitro and in vivo. Whatever the reason, these results underscore the importance of in vivo assays to determine the true impact on the virulence of mycobacterial permeability defects detected in vitro.

By combining a variety of infection models with in vitro assays, we have demonstrated that the *Mycobacterium erp* locus is required for intracellular growth and survival and that this requirement may be due in part to its role in maintaining integrity of the cell wall and outer lipid layer. The use of *M. marinum* as a surrogate model in the zebrafish has allowed a more precise determination of this attenuation defect than was previously apparent.

ACKNOWLEDGMENTS

We thank Hannah Volkman for assistance with embryo infections; Muse Davis for assistance with figures; Richard Burmeister for artwork; Eric Brown for *M. marinum* strains; and Lynn Connolly, Hannah Volkman, David Sherman, and Yong Gao for comments on the manuscript.

This study was supported by NIH grants RO1 AI036396 and RO1 AI54503 to L.R.

REFERENCES

1. **Aronson, J. D.** 1926. Spontaneous tuberculosis in salt water fish. J. Infect. Dis. **39:**315–320.
2. **Banu, S., N. Honore, B. Saint-Joanis, D. Philpott, M. C. Prevost, and S. T. Cole.** 2002. Are the PE-PGRS proteins of *Mycobacterium tuberculosis* variable surface antigens? Mol. Microbiol. **44:**9–19.
3. **Barker, L. P., K. M. George, S. Falkow, and P. L. Small.** 1997. Differential trafficking of live and dead *Mycobacterium marinum* organisms in macrophages. Infect. Immun. **65:**1497–1504.
4. **Berthet, F. X., M. Lagranderie, P. Gounon, C. Lauren-Winter, D. Ensergueix, P. Chavarot, F. Thouron, E. Maranghi, V. Pelicic, D. Portnoi, G. Marchal, and B. Gicquel.** 1998. Attenuation of virulence by disruption of the *Mycobacterium tuberculosis erp* gene. Science **282:**759–762.
5. **Bigi, F., A. Gioffre, L. Klepp, M. P. Santangelo, C. A. Velicovsky, G. H. Giambartolomei, C. A. Fossati, M. I. Romano, T. Mendum, J. J. McFadden, and A. Cataldi.** 2005. Mutation in the P36 gene of *Mycobacterium bovis* provokes attenuation of the bacillus in a mouse model. Tuberculosis **85:**221–226.
6. **Bouley, D. M., N. Ghori, K. L. Mercer, S. Falkow, and L. Ramakrishnan.** 2001. Dynamic nature of host-pathogen interactions in *Mycobacterium marinum* granulomas. Infect. Immun. **69:**7820–7831.
7. **Brennan, M. J., G. Delogu, Y. Chen, S. Bardarov, J. Kriakov, M. Alavi, and W. R. Jacobs, Jr.** 2001. Evidence that mycobacterial PE_PGRS proteins are cell surface constituents that influence interactions with other cells. Infect. Immun. **69:**7326–7333.
8. **Camacho, L. R., P. Constant, C. Raynaud, M. A. Laneelle, J. A. Triccas, B. Gicquel, M. Daffe, and C. Guilhot.** 2001. Analysis of the phthiocerol dimycocerosate locus of *Mycobacterium tuberculosis*: evidence that this lipid is involved in the cell wall permeability barrier. J. Biol. Chem. **276:**19845–19854.
9. **Camacho, L. R., D. Ensergueix, E. Perez, B. Gicquel, and C. Guilhot.** 1999. Identification of a virulence gene cluster of *Mycobacterium tuberculosis* by signature-tagged transposon mutagenesis. Mol. Microbiol. **34:**257–267.
10. **Chan, K., T. Knaak, L. Satkamp, O. Humbert, S. Falkow, and L. Ramakrishnan.** 2002. Complex pattern of *Mycobacterium marinum* gene expression during long-term granulomatous infection. Proc. Natl. Acad. Sci. USA **99:**3920–3925.
11. **Converse, S. E., J. D. Mougous, M. D. Leavell, J. A. Leary, C. R. Bertozzi, and J. S. Cox.** 2003. MmpL8 is required for sulfolipid-1 biosynthesis and *Mycobacterium tuberculosis* virulence. Proc. Natl. Acad. Sci. USA **100:**6121–6126.
12. **Cosma, C. L., J. M. Davis, L. E. Swaim, H. Volkman, and L. Ramakrishnan.** Animal models of *Mycobacterium marinum* infection. Curr. Protocols Microbiol., in press.
13. **Cosma, C. L., D. R. Sherman, and L. Ramakrishnan.** 2003. The secret lives of the pathogenic mycobacteria. Annu. Rev. Microbiol. **57:**641–676.
14. **Cox, J. S., B. Chen, M. McNeil, and W. R. Jacobs, Jr.** 1999. Complex lipid determines tissue-specific replication of *Mycobacterium tuberculosis* in mice. Nature **402:**79–83.
15. **Davis, J. M., H. Clay, J. L. Lewis, N. Ghori, P. Herbomel, and L. Ramakrishnan.** 2002. Real-time visualization of *Mycobacterium*-macrophage interactions leading to initiation of granuloma formation in zebrafish embryos. Immunity **17:**693–702.
16. **De Mendonca-Lima, L., Y. Bordat, E. Pivert, C. Recchi, O. Neyrolles, A. Maitournam, B. Gicquel, and J.-M. Reyrat.** 2003. The allele encoding the mycobacterial Erp protein affects lung disease in mice. Cell. Microbiol. **5:**65–73.
17. **De Mendonca-Lima, L., M. Picardeau, C. Raynaud, J. Rauzier, Y. O. de la Salmoniere, L. Barker, F. Bigi, A. Cataldi, B. Gicquel, and J. M. Reyrat.** 2001. Erp, an extracellular protein family specific to mycobacteria. Microbiology **147:**2315–2320.
18. **Dionne, M. S., N. Ghori, and D. S. Schneider.** 2003. *Drosophila melanogaster* is a genetically tractable model host for *Mycobacterium* marinum. Infect. Immun. **71:**3540–3550.
19. **Domenech, P., M. B. Reed, and C. E. Barry III.** 2005. Contribution of the *Mycobacterium tuberculosis* MmpL protein family to virulence and drug resistance. Infect. Immun. **73:**3492–3501.
20. **Dubnau, E., J. Chan, C. Raynaud, V. P. Mohan, M. A. Laneelle, K. Yu, A. Quemard, I. Smith, and M. Daffe.** 2000. Oxygenated mycolic acids are necessary for virulence of *Mycobacterium tuberculosis* in mice. Mol. Microbiol. **36:**630–637.
21. **Gao, L. Y., S. Guo, B. McLaughlin, H. Morisaki, J. N. Engel, and E. J. Brown.** 2004. A mycobacterial virulence gene cluster extending RD1 is required for cytolysis, bacterial spreading, and ESAT-6 secretion. Mol. Microbiol. **53:**1677–1693.
22. **Gao, L. Y., F. Laval, E. H. Lawson, R. K. Groger, A. Woodruff, J. H. Morisaki, J. S. Cox, M. Daffe, and E. J. Brown.** 2003. Requirement for *kasB* in *Mycobacterium* mycolic acid biosynthesis, cell wall impermeability and intracellular survival: implications for therapy. Mol. Microbiol. **49:**1547–1563.
23. **Glickman, M. S., J. S. Cox, and W. R. Jacobs, Jr.** 2000. A novel mycolic acid cyclopropane synthetase is required for cording, persistence, and virulence of *Mycobacterium tuberculosis*. Mol. Cell **5:**717–727.
24. **Glickman, M. S., and W. R. Jacobs, Jr.** 2001. Microbial pathogenesis of *Mycobacterium tuberculosis*: dawn of a discipline. Cell **104:**477–485.
25. **Guinn, K. M., M. J. Hickey, S. K. Mathur, K. L. Zakel, J. E. Grotzke, D. M. Lewinsohn, S. Smith, and D. R. Sherman.** 2004. Individual RD1-region genes are required for export of ESAT-6/CFP-10 and for virulence of *Mycobacterium tuberculosis*. Mol. Microbiol. **51:**359–370.
26. **Hsu, T., S. M. Hingley-Wilson, B. Chen, M. Chen, A. Z. Dai, P. M. Morin, C. B. Marks, J. Padiyar, C. Goulding, M. Gingery, D. Eisenberg, R. G. Russell, S. C. Derrick, F. M. Collins, S. L. Morris, C. H. King, and W. R. Jacobs, Jr.** 2003. The primary mechanism of attenuation of bacillus Calmette-Guerin is a loss of secreted lytic function required for invasion of lung interstitial tissue. Proc. Natl. Acad. Sci. USA **100:**12420–12425.
27. **Jackson, M., C. Raynaud, M. A. Laneelle, C. Guilhot, C. Laurent-Winter, D. Ensergueix, B. Gicquel, and M. Daffe.** 1999. Inactivation of the antigen 85C gene profoundly affects the mycolate content and alters the permeability of the *Mycobacterium tuberculosis* cell envelope. Mol. Microbiol. **31:**1573–1587.
28. **Jain, M., and J. S. Cox.** 2005. Interaction between polyketide synthase and transporter suggests coupled synthesis and export of virulence lipid in *M. tuberculosis*. PLoS Pathogens **1:**12–19.
29. **Kocincova, D., B. Sonden, Y. Bordat, E. Pivert, L. de Mendonca-Lima, B. Gicquel, and J.-M. Reyrat.** 2004. The hydrophobic domain of the mycobacterial Erp protein is not essential for the virulence of *Mycobacterium tuberculosis*. Infect. Immun. **72:**2379–2382.
30. **Kocincova, D., B. Sonden, L. de Mendonca-Lima, B. Gicquel, and J.-M. Reyrat.** 2004. The Erp protein is anchored at the surface by a carboxy-terminal hydrophobic domain and is important for cell wall structure in *Mycobacterium smegmatis*. FEMS Microbiol. Lett. **231:**191–196.
31. **Lewis, K. N., R. Liao, K. M. Guinn, M. J. Hickey, S. Smith, M. A. Behr, and D. R. Sherman.** 2003. Deletion of RD1 from *Mycobacterium tuberculosis* mimics BCG attenuation. J. Infect. Dis. **187:**117–123.
32. **McKinney, J. D.** 2000. In vivo veritas: the search for TB drug targets goes live. Nat. Med. **6:**1330–1333.
33. **Meijer, A. H., F. J. Verbeek, E. Salas-Vidal, M. Corredor-Adamez, J. Bussman, A. M. van der Sar, G. W. Otto, R. Geisler, and H. P. Spaink.** 2005. Transcriptome profiling of adult zebrafish at the late stage of chronic tuberculosis due to *Mycobacterium marinum* infection. Mol. Immunol. **42:**1185–1203.
34. **Pozos, T. C., and L. Ramakrishnan.** 2004. New models for the study of *Mycobacterium*-host interactions. Curr. Opin. Immunol. **16:**499–505.
35. **Pym, A. S., P. Brodin, R. Brosch, M. Huerre, and S. T. Cole.** 2002. Loss of RD1 contributed to the attenuation of the live tuberculosis vaccines *Mycobacterium bovis* BCG and *Mycobacterium microti*. Mol. Microbiol. **46:**709–717.
36. **Ramakrishnan, L., N. A. Federspiel, and S. Falkow.** 2000. Granuloma-specific expression of *Mycobacterium* virulence proteins from the glycine-rich PE-PGRS family. Science **288:**1436–1439.
37. **Ramakrishnan, L., R. H. Valdivia, J. H. McKerrow, and S. Falkow.** 1997. *Mycobacterium marinum* causes both long-term subclinical infection and acute disease in the leopard frog (*Rana pipiens*). Infect. Immun. **65:**767–773.

38. **Rousseau, C., N. Winter, E. Pivert, Y. Bordat, O. Neyrolles, P. Ave, M. Huerre, B. Gicquel, and M. Jackson.** 2004. Production of phthiocerol dimycocerosates protects *Mycobacterium tuberculosis* from the cidal activity of reactive nitrogen intermediates produced by macrophages and modulates the early immune response to infection. Cell. Microbiol. **6:**277–287.
39. **Sassetti, C. M., and E. J. Rubin.** 2003. Genetic requirements for mycobacterial survival during infection. Proc. Natl. Acad. Sci. USA **100:**12989–12994.
40. **Sherman, D. R., M. Voskuil, D. Schnappinger, R. Liao, M. I. Harrell, and G. K. Schoolnik.** 2001. Regulation of the *Mycobacterium tuberculosis* hypoxic response gene encoding alpha-crystallin. Proc. Natl. Acad. Sci. USA **98:** 7534–7539.
41. **Smith, I.** 2003. *Mycobacterium tuberculosis* pathogenesis and molecular determinants of virulence. Clin. Microbiol. Rev. **16:**463–496.
42. **Solomon, J. M., G. Leung, and R. R. Isberg.** 2003. Intracellular replication of *Mycobacterium marinum* within *Dictyostelium discoideum*: efficient replication in the absence of host coronin. Infect. Immun. **71:**3578–3586.
43. **Tonjum, T., D. B. Welty, E. Jantzen, and P. L. Small.** 1998. Differentiation of *Mycobacterium ulcerans*, *M. marinum*, and *M. haemophilum*: mapping of their relationships to *M. tuberculosis* by fatty acid profile analysis, DNA-DNA hybridization, and 16S rRNA gene sequence analysis. J. Clin. Microbiol. **36:**918–925.
44. **Travis, W. D., L. B. Travis, G. D. Roberts, D. W. Su, and L. W. Weiland.** 1985. The histopathologic spectrum in *Mycobacterium marinum* infection. Arch. Pathol. Lab. Med. **109:**1109–1113.
45. **Volkman, H. E., H. Clay, D. Beery, J. C. Chang, D. R. Sherman, and L. Ramakrishnan.** 2004. Tuberculous granuloma formation is enhanced by a *Mycobacterium* virulence determinant. PLoS Biol. **2:**1946–1956.

Editor: J. L. Flynn